Acta Biochim Biophys Sin 2023, 55(3): 382–393
https://doi.org/10.3724/abbs.2023037
Advance Access Publication Date: 23 March 2023
Original Article

Original Article

Roles of the hsa_circ_0013880/USP32/Rap1b axis in the proliferation and apoptosis of acute myeloid leukemia cells

Heyang Zhang, Yuan Tao, Xin Ding, Yue Wang, and Xiaoxue Wang*

Department of Hematology, the First Hospital of China Medical University, Shenyang 110000, China
*Correspondence address. Tel: +86-24-83282501; E-mail: liang195691@163.com

Received 28 March 2022 Accepted 7 August 2022

Abstract

Acute myeloid leukemia (AML) is a myeloid malignancy with generally high mortality. Although recent advances in AML research have revealed that circRNAs play significant roles in AML progression, our understanding of the leukemogenic mechanism of circRNAs remains very limited. In this study, increased expression of hsa_circ_0013880 was observed in bone marrow mononuclear cells (BMNCs) of AML patients. Overexpression of hsa_circ_0013880 promotes AML cell proliferation and migration and reduces cell apoptosis. Mechanistically, hsa_circ_0013880 could elevate the expression of USP32, a deubiquitinating enzyme that is highly expressed in the BMNCs of AML patients. Given the deubiquitination function of USP32, we further hypothesize that USP32 may mediate the malignant behaviors of AML cells by regulating the stability of Ras-related protein (Rap1b). At the molecular level, we find that silencing of *USP32* increases ubiquitinated Rap1b. Overexpression of Rap1b restores the effects of *USP32* knockdown, which further verifies our hypothesis. In addition, we propose another hypothesis that a potential regulatory network among hsa_circ_0013880, miR-148a-3p/miR-20a-5p and USP32 might exist in the development of AML, according to bioinformatics website predictions and our preliminary experimental verification. Overall, our findings will enrich the understanding of the hsa_circ_0013880/USP32/Rap1b axis in AML development, which may contribute to the development of novel therapeutic strategies for AML.

Key words hsa_circ_0013880, USP32, Rap1b, acute myeloid leukemia

Introduction

Acute myeloid leukemia (AML), a common hematological malignancy with high heterogeneity, is characterized by the accumulation of undifferentiated myeloid blasts and abnormal bone marrow stromal cells in the bone marrow and peripheral blood [1]. As the mechanistic underpinnings are gradually clarified, the US Food and Drug Administration (FDA) has approved 10 agents for different AML indications since 2017 [2]. Despite advances in the development of targeted therapeutics, the overall prognosis of AML patients, especially in elderly patients (usually older than 60 years of age), remains dismal [3,4]. Therefore, there is an urgent need to explore innovative diagnostic biomarkers or therapeutic targets for improving the outcome in treatment of AML patients.

Circular RNAs (circRNAs) are a novel class of endogenous noncoding RNAs with a covalently closed loop structure [5]. Due to advances in sequencing technology, an increasing number of circRNAs have been identified to be involved in the development of AML [6,7]. For example, according to a circRNA microarray analysis that was performed on six newly diagnosed cytogenetically normal AML (CN-AML) patients and four healthy controls, 464 differentially expressed circRNAs (147 upregulated and 317 downregulated) were found in CN-AML patients based on whether they had FLT3-ITD and NPM1 mutations [8]. Hsa_circ_0013880 (circBase ID: hsa_circ_0013880), a circRNA located at chr1: 145439592-145442628, caught our attention. Its gene symbol is thioredoxin interacting protein (*TXNIP*) [9]. However, no data have been reported regarding the exact expression and function of hsa_circ_0013880 in AML.

Ubiquitination refers to the covalent posttranslational modification of substrate proteins by ubiquitin molecules, which controls protein degradation, alters protein localization, and prevents or promotes protein interactions [10,11]. In contrast, deubiquitinating enzymes (DUBs) reverse the role of ubiquitination by removing ubiquitin from substrates [12]. USP32, a member of the ubiquitin-specific protease family, was reported to be a key DUB in guarding the health of the endolysosomal system by deubiquitination of Rab7

[13]. Previous studies also reported that USP32 is involved in the pathogenesis of various cancers [13–15]. For example, USP32 functions as an oncogene in gastric carcinoma via upregulation of SMAD2 [14]. Knockdown of *USP32* significantly decreases the proliferation and migration rates of human small cell lung cancer [15]. Recently, a DUB-screening analysis performed on breast cancer cells revealed a resistance mechanism governed by USP32, which is related to YM155 (Sepantronium Bromide) resistance [16]. Nevertheless, the role of USP32 in AML remains obscure.

In this study, the relative expression of hsa_circ_0013880 was first revealed in AML patients and cell lines, and correlation analysis of the expression of hsa_circ_0013880 and USP32 was performed at the mRNA level. Given the deubiquitination function of USP32, we then reasonably hypothesized that USP32 might contribute to the progression of AML by stabilizing Ras-related protein (Rap1b). Collectively, our findings indicated the possibility that the hsa_circ_0013880/USP32/Rap1b axis might serve as a novel therapeutic target for AML.

Materials and Methods

Patients and samples

Eighteen patients with AML and 17 age-matched healthy donors (control group), with informed consent, were enrolled in this study from the First Hospital of China Medical University (Shenyang, China). This study was approved by the Ethics Committee of the First Hospital of China Medical University and followed the guidelines of the Helsinki Declaration. All patients in this study were newly diagnosed with AML. Bone marrow mononuclear cells (BMNCs) were isolated from the bone marrow aspirate of patients for analysis of hsa_circ_0013880, USP32, miR-148a-3p, miR-20a-5p and Rab1b expression levels. BMNCs were randomly selected from 5 AML patients and 5 healthy donors for the detection of USP32 and Rab1b protein levels. The medical records of AML patients with clinical staging are summarized in Supplementary Table S1.

Cells and chemical reagents

HL-60 and U937 AML cell lines were purchased from Procell Life Science & Technology (Wuhan, China). IMDM medium (Procell Life Science & Technology) supplemented with 20% fetal bovine serum (FBS; Tianhang, Zhejiang, China) and RPMI-1640 medium (Solarbio Science & Technology, Beijing, China) supplemented with 10% FBS were used to culture HL-60 and U937 cells, respectively. All cells were cultured in an incubator with 5% CO_2 at 37°C. Cycloheximide (CHX, protein synthesis inhibitor) was purchased from MedChemExpress (Shanghai, China), and MG132 (proteasome inhibitor) was purchased from Aladdin Regents (Shanghai, China).

Lentiviral infection and plasmid transfection

For overexpression of hsa_circ_0013880, lentivirus expressing hsa_circ_0013880 (LV-Circ) and its control (LV-vec) were packaged to infect HL-60 cells. hsa_circ_0013880-overexpressing plasmids were constructed in pLC5-ciR vector (GS0108; Geneseed, Guangzhou, China) by Genscript Biotechnology (Nanjing, China). Small interference (Si) RNA against hsa-circ-0013880 (Si1-Circ and Si2-Circ) and its negative control (si-NC) were synthesized by General Biol (Chuzhou, China). The sequences targeting hsa-circ-0013880 are as follows: Si1 (sense, 5′-UGGAAGUGAGAAUGAGAUGGU-3′; antisense, 5′-ACCAUCUCAUUCUCACUUCCA-3′) and Si2 (sense, 5′-UAAUGGAAGUGAGAAUGAGAU-3′; antisense, 5′-AUCUCAUUCUCACUUCCAUUA-3′). miR-148a-3p/NC mimics, miR-20a-5p mimics/NC, miR-148a-3p/NC inhibitor, and miR-20a-5p/NC inhibitor were purchased from General Biol. The sequences used for the microRNA mimics or inhibitors are as follows: miR-148a-3p mimics (sense, 5′-UCAGUGCACUACAGAACUUUGU-3′; antisense, 5′-ACAAAGUUCUGUAGUGCACUGA-3′), miR-20a-5p mimics (sense, 5′-UAAAGUGCUUAUAGUGCAGGUAG-3′; antisense, 5′-CUACCUGCACUAUAAGCACUUUA-3′), miR-148a-3p inhibitor (5′-ACAAAGUUCUGUAGUGCACUGA-3′) and miR-20a-5p inhibitor (5′-CUACCUGCACUAUAAGCACUUUA-3′). For silencing of *USP32*, the target mRNA sequences (sh#1, 5′-GAGGAGAGUUACAGAUGUAGA-3′; sh#2, 5′-GGAUCUCUCUGAUAUUGUAGA-3′) were designed, synthesized, and cloned into pLVX-shRNA1 vector (BR004) by Genscript Biotechnology. HL-60 and U937 cells were collected, seeded and then infected with USP32 shRNA lentiviruses (LV-USP32sh#1 and LV-USP32sh#2) or control shRNA lentiviruses (LV-shCtrl). The pLVX-IRES-puro and pLVX-shRNA1 vectors were obtained from Fenghui Biotechnology (Changsha, China). For overexpression of Rap1b, lentivirus expressing Rap1b (LV-Rap1b) and its control (OE-vec) were constructed to infect HL-60 cells. Rap1b-overexpressing plasmids were constructed in pLVX-IRES-puro vector (BR025) by Genscript Biotechnology. According to the manufacturer's instructions, the Lipofectamine™ 3000 reagent (Invitrogen, Carlsbad, USA) was used for plasmid transfection. Real-time PCR and western blot analysis were performed to evaluate the transfection efficiency.

Dual-luciferase reporter assay

Based on the bioinformatics analysis performed on the Bielefeld Bioinformatics Server (BiBiServ, https://bibiserv.cebitec.uni-bielefeld.de/), miR-148a-3p and miR-20a-5p were predicted to be the downstream targets for hsa_circ_0013880. USP32 was predicted to be a downstream target for miR-148a-3p and miR-20a-5p. To further verify these predictions, the 3′-UTR or mutant sequences of USP32 mRNA (wt-USP32 or mut-USP32) and the fragments of wild-type (wt)-hsa_circ_0013880 and mut-hsa_circ_0013880 were cloned into the pmirGLO vectors (General Biol). For luciferase assay, pmirGLO vectors (pmirGLO-wt-USP32, pmirGLO-mut-USP32, pmirGLO-wt-hsa_circ_0013880 or pmirGLO-mut-hsa_circ_0013880) and miRNA mimics (miR-148a-3p/NC mimics or miR-20a-5p/NC mimics) were cotransfected into 293T cells. After 48 h, the luciferase activities were detected by using a dual luciferase reporter gene assay kit (KeyGEN, Nanjing, China).

Characterization of hsa_circ_0013880

Genomic DNA (gDNA) was extracted by using a gDNA extraction kit (BioTeke, Beijing, China). hsa_circ_0013880 was further characterized on either cDNA or gDNA templates by using either divergent primers that amplify only circular transcripts or convergent primers that detect linear RNA molecules. The products were subjected to agarose gel electrophoresis. For the RNase R digestion assay, the extracted RNA was treated with RNase R (Geneseed) and then reverse transcribed to cDNA using random primers. The levels of hsa_circ_0013880 and TXNIP were detected by real-time PCR. The sequences of the primers are as follows: convergent primers (forward, 5′-CAGACCAAGGTGCTGACTC-3′, and reverse, 5′-CCAGGAACGCTAACATAGA-3′) and divergent primers (forward, 5′-AGCCATAGCACTTTGTTC-3′, and reverse, 5′-ATTTGTTTCCAGGTCTCA-3′).

Real-time qPCR

To analyse USP32, Rap1b and hsa_circ_0013880 expressions, TRIpure reagent (BioTeke) was added to the cells to extract total RNA. cDNA was acquired using BeyoRT™ II M-MLV Reverse Transcriptase (Beyotime Biotechnology, Shanghai, China) in accordance with the manufacturer's instructions. For the analysis of microRNAs, total RNAs were isolated from cells by using an RNA simple total RNA kit (TIANGEN BIOTECH, Beijing, China) and reverse-transcribed by using a miRNA First Strand cDNA Synthesis (Tailing Reaction) kit (B532451; Sangong Biotech, Shanghai, China) following the manufacturer's instructions. Quantitative real-time PCR was carried out by using the Exicycler™ 96 machine (Bioneer, Daejeon, Korea) in a 20 μL reaction system containing 1 μL of cDNA, 0.3 μL of SYBR green, 10 μL of 2 × Taq PCR MasterMix (Solarbio Science & Technology), 0.5 μL of forwards primer and 0.5 μL of reverse primer. The real-time PCR amplification procedure incudes: 5 min at 94°C for pre-denaturation; 40 cycles in 94°C for denaturation (10 s), 60°C for annealing (20 s) and 72°C for extension (30 s). The primer sequences are as follows: *hsa_circ_0013880* (forward: 5′-AGCCATAGCACTTTGTTC-3′, reverse: 5′-ATTTGTTTCCAGGTCTCA-3′); *USP32* (forward: 5′-CACCTATTC GTCCATCT-3′, reverse: 5′-ATCACGGTCAACATCAA-3′); *Rap1b* (forward: 5′-GTAGGGAAGGAACAAGGT-3′, reverse: 5′-GCCGCACT AGGTCATAAA-3′); *miR-148a-3p* (forward: 5′-TCAGTGCACTACAG AACTTTGT-3′); and *miR-20a-5p* (forward: 5′-TAAAGTGCTTAT AGTGCAGGTAG-3′). The reverse primers of microRNAs were contained in the miRNA First Strand cDNA Synthesis (Tailing Reaction) kit. The $2^{-\Delta CT}$ and $2^{-\Delta\Delta CT}$ methods were used to calculate the relative expression of targets in BMNCs from patients and cultured AML cells, respectively.

Western blot analysis

Cells were lysed in cell lysis buffer (Beyotime Biotechnology) containing 1 mM PMSF (Beyotime Biotechnology). The cell lysates were then centrifuged at 10,000 *g* for 5 minutes at 4°C. After collecting the cell supernatants, a BCA assay kit (Beyotime Biotechnology) was used to determine the protein concentration. Protein samples were separated by sodium dodecyl sulfate (SDS)-polyacrylamide gel electrophoresis and transferred onto PVDF membranes (Millipore, Billerica, USA). To inhibit nonspecific binding, the membranes were blocked in 5% nonfat milk dissolved in TBST buffer for 1 h. Subsequently, the membranes were incubated overnight with the corresponding primary antibodies at 4°C. After wash with TBST buffer four times, the membranes were incubated with HRP-labelled secondary antibodies diluted 1:5000 in 5% (M/V) nonfat milk for 45 minutes at 37°C. Protein bands were visualized with ECL chemiluminescence western blotting detection reagents (Beyotime Biotechnology). Signals were quantified with Gel-Pro-Analyzer software. The antibodies used in this study are as follows: USP32 (1:500; Proteintech, Rosemont, USA), Cyclin D1 (1:400; ABclonal Technology, Wuhan, China), cleaved caspase-3 (1:500; Affbiotech, Changzhou, China), CDK4 (1:500; ABclonal Technology), P21 (1:1000; ABclonal Technology), cleaved caspase-9 (1:1000; CST, Danvers, USA), cleaved PARP (1:500; CST), Rap1b (1:1000; Proteintech), β-actin (Santa Cruz Biotechnology, Santa Cruz, USA), HRP-labelled goat anti-rabbit IgG (Beyotime Biotechnology), HRP-labelled goat anti-mouse IgG (Beyotime Biotechnology). β-Actin was used as the protein loading control.

Determination of caspase-3 and caspase-9 activities

The activity of caspase-3 and caspase-9 was determined using the caspase-3 activity assay kit (Beyotime Biotechnology) and the caspase-9 activity assay kit (Beyotime Biotechnology) respectively according to the manufacturer's protocol. Briefly, cell lysates were prepared and incubated with Ac-DEVD-pNA (caspase-3 substrate) or Ac-LEHD-pNA (caspase-9 substrate) in reaction buffer for 2–4 h at 37°C. Caspase activity was measured by cleavage of the corresponding Ac-DEVD-pNA or Ac-LEVD-pNA into p-nitroanilide (pNA). The absorbance was detected at 405 nm with a microplate reader (ELX-800; BioTek Instruments, Winooski, USA).

Cell viability assay

The cell counting kit-8 (CCK-8; Solarbio Science & Technology) were used to quantitatively evaluate cell viability. HL-60 cells were seeded in 96-well culture plates and infected with the indicated lentiviral particles for 48 h. Then, 10 μL of CCK-8 solution was added into each well and incubated at 37°C for 2 h. In addition, HL-60 and U937 cells transfected with NC-shRNA or USP32-shRNAs were reseeded in 96-well plates and incubated for 72 h at 37°C in an incubator with 5% CO_2. Every 24 h interval, CCK-8 solution (10 μL) was added to each well and incubated at 37°C for 2 h. The absorbances were recorded at 450 nm with a microplate absorbance reader (800TS; BioTek Instruments).

Cell apoptosis analysis

Cell apoptosis was assayed by using an Annexin V-APC/PI apoptosis detection kit (KeyGEN) following the manufacturer's guidelines. After infection with the indicated lentiviral particles for 48 h, HL-60 and U937 cells were harvested and centrifuged at 300 *g* for 5 minutes. Afterwards, the cells were washed twice with PBS and incubated with Annexin V-APC/PI at room temperature for 15 minutes in the dark. The fluorescence of the cells was detected with a NovoCyte flow cytometer (ACEA Biosciences, San Diego, USA). Early and late apoptotic cells were identified by Annexin V-APC^+/PI^- and Annexin V-APC^+/PI^+ staining.

Transwell migration assay

Migration assays were carried out in triplicate using 8-μm pore-size transwells (LABSELECT, Beijing, China). The lower compartment contained 800 μL culture medium containing 10% FBS. HL-60 cell suspensions (200 μL) were added to the upper compartment and allowed to migrate for 24 h. The quantified results are shown as the number of cells that migrated to the lower compartment.

Colony-forming unit assay

HL-60 and U937 cells infected with the indicated lentiviral particles were plated in petri dishes that contained medium supplemented with 0.8% methylcellulose (Aladdin Regents). Initially, 500 cells were seeded in each petri dish. After 14 days of culture, colony numbers in each petri dish were directly quantified.

Cell cycle analysis

Cell cycle and apoptosis analysis kits purchased from Beyotime Biotechnology were used to analyse cell cycle progression. HL-60 and U937 cells were fixed in prechilled 70% methanol and incubated at 4°C for 12 h. After fixation, the cells were collected and washed with PBS 2 times. After centrifugation, cell pellets were fully resuspended in 500 μL staining buffer, which contained 25 μL

PI and 10 μL RNase A. After incubation in the dark for 30 min, analysis was performed on a NovoCyte flow cytometer (ACEA Biosciences).

Ubiquitination assay

HL-60 and U937 cells were infected with the indicated lentiviral particles and pretreated with 10 μM MG132 for 8 h. Subsequently, cells were harvested and lysed in lysis buffer (Beyotime Biotechnology) containing 1 mM PMSF (Beyotime Biotechnology). The ubiquitination status of Rap1b was assessed by immunoprecipitation with an anti-Rap1b antibody and immunoblotting with a ubiquitin rabbit mAb (ABclonal Technology) or anti-Rap1b antibody.

Statistical analysis

Data were processed using GraphPad Prism 8.0 (GraphPad Software, San Diego, USA) and shown as the mean ± SD. The correlation between hsa_circ_0013880 and USP32 expression in AML patients was analysed by Pearson's test. Statistical evaluations between two groups were performed by two-tailed Student's *t* test. Multiple comparisons were performed using one-way ANOVA followed by Tukey's post hoc test. $P < 0.05$ was considered statistically significant.

Results

hsa_circ_0013880 and USP32 were upregulated in AML patients

hsa_circ_0013880 is located at chr1:145439592-145442628 (Figure 1A). To explore the characteristics of hsa_circ_0013880, we designed divergent primers and convergent primers to amplify hsa_circ_0013880. As shown in Figure 1B, convergent primers amplified both cDNA and gDNA, while divergent primers detected circular RNAs in cDNA but not in gDNA. Moreover, linear TXNIP was degraded by RNase R, while hsa_circ_0013880 was resistant to RNase R degradation, suggesting that hsa_circ_0013880 was more stable than TXNIP (Figure 1C). Furthermore, real-time PCR was performed to evaluate the biological significance of hsa_circ_0013880 in AML. The results showed that hsa_circ_0013880 was highly expressed in BMNCs from AML patients (Figure 1D). Importantly, the mRNA level of USP32 was also upregulated in AML patients compared with healthy individuals (Figure 1E), which was positively correlated with hsa_circ_0013880 expression (Figure 1F). Western blot analysis also verified that the protein expression of USP32 was consistently increased in AML patients (Supplementary Figure S1).

Potential association of hsa_circ_0013880, miR-148a-3p/miR-20a-5p and USP32 in HL-60 cells

The online public Bioinformatics (TargetScan) predictions suggested that USP32 might be a potential target for miR-148a-3p and miR-20a-5p. The results of the luciferase reporter assay showed that the luciferase activity was significantly lower in pmirGLO-wt-USP32 cells transfected with miR-148a-3p or miR-20a-5p mimics than in the pmirGLO-wt-USP32 and NC mimic groups (Figure 2A). Next, we treated HL-60 cells with miR-148a-3p or miR-20a-5p inhibitors to downregulate the expression of these two microRNAs (Figure 2B,C). Real-time PCR assays showed that silencing of miR-148a-3p and miR-20a-5p could increase USP32 expression (Figure 2D,E). These findings suggested that miR-148a-3p and miR-20a-5p mediated USP32 expression by targeting its 3′-UTR. Furthermore, through Bielefeld BioInformatics Service (BiBiServ) prediction, we discovered that hsa_circ_0013880 could bind to miR-148a-3p and miR-20a-5p. Dual-luciferase reporter assays verified that cotransfection

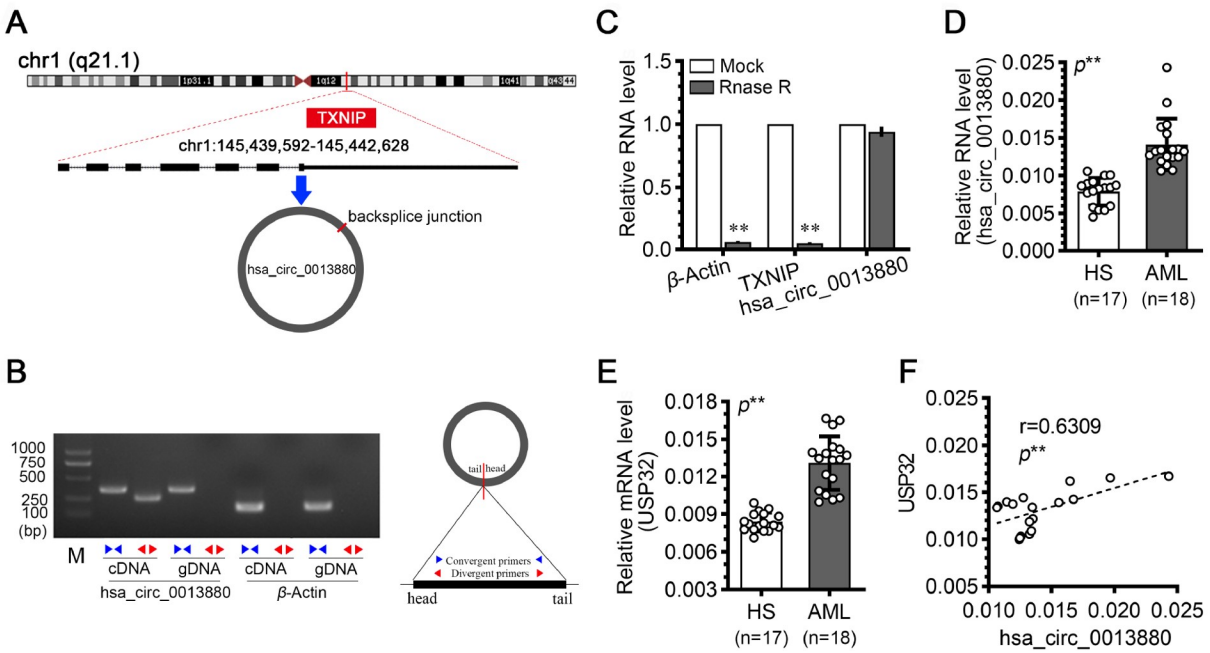

Figure 1. Hsa_circ_0013880 and USP32 were highly expressed in bone marrow mononuclear cells (BMNCs) of AML patients (A) hsa_circ_0013880 is located at chr1: 145439592-145442628, and its gene symbol is thioredoxin interacting protein (TXNIP). (B) Convergent and divergent primers were used to verify the closed loop structure of hsa_circ_0013880. (C) Amplification of hsa_circ_0013880 and TXNIP after RNase R treatment. (D,E) The relative RNA/mRNA levels of hsa_circ_0013880 and USP32 were detected by real-time PCR. (F) Correlation of hsa_circ_0013880 and USP32 in AML patients. $^{**}P < 0.01$. Data are presented as the mean ± SD. M, marker; HS, healthy samples.

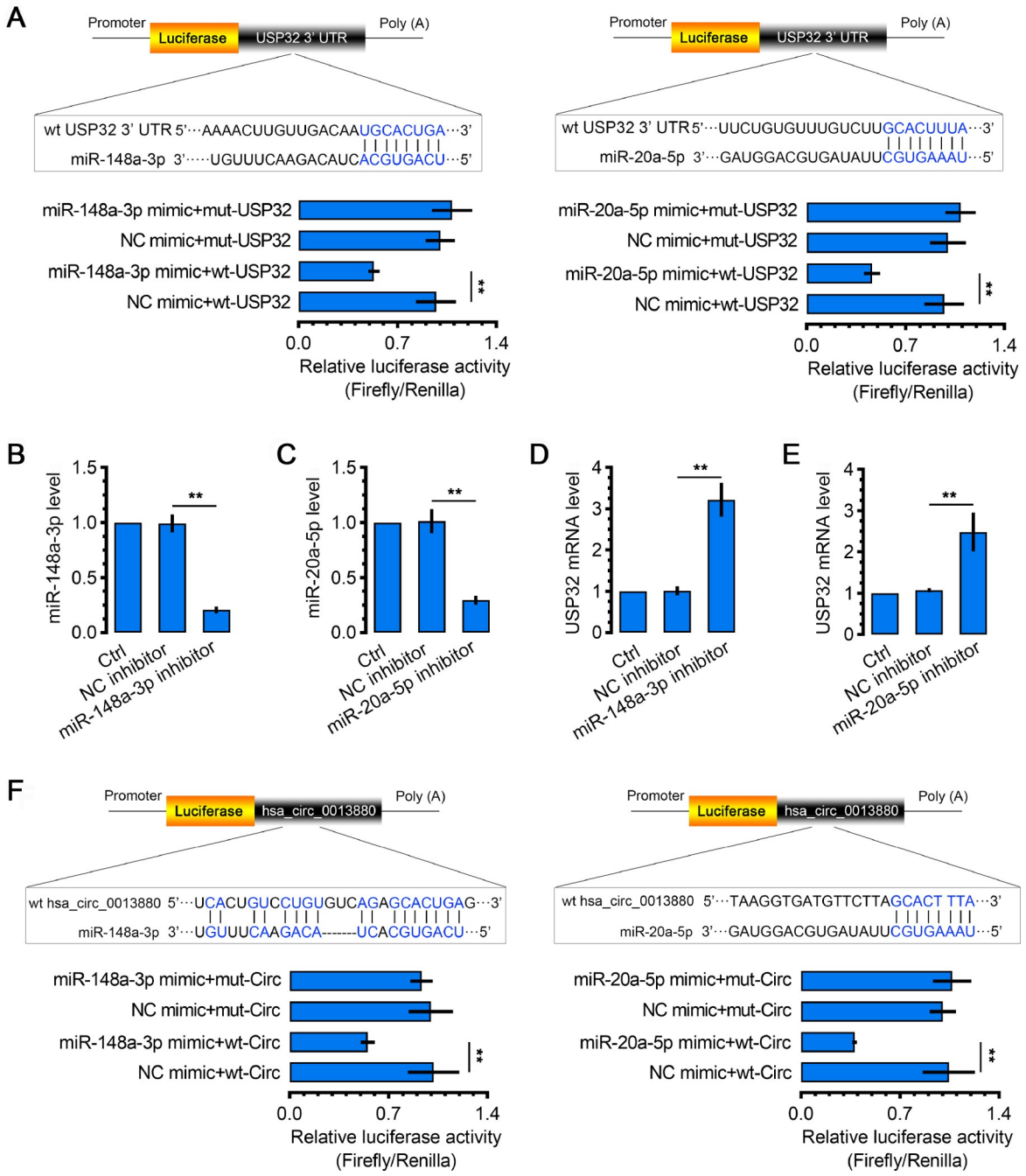

Figure 2. Bioinformatics predictions and dual-luciferase validation assays performed on HL-60 cells (A) A dual-luciferase assay was performed to verify the binding between USP32 and miR-148a-3p or miR-20a-5p. (B,C) Real-time PCR was used to evaluate the knockdown efficiency of miR-148a-3p or miR-20a-5p. (D,E) The mRNA level of *USP32* was detected by real-time PCR following microRNA downregulation. (F) Dual-luciferase assay was performed to verify the binding between hsa-circ-0013880 and miR-148a-3p or miR-20a-5p. For dual-luciferase assay, 293T cells were cotransfected with pmirGLO-wt-hsa_circ_0013880, pmirGLO-mut-hsa_circ_0013880, pmirGLO-wt-USP32 and pmirGLO-mut-USP32, along with miR-148a-3p/NC mimics or miR-20a-5p/NC mimics. $^{**}P < 0.01$. Data are presented as the mean ± SD. Ctrl, control parental cells.

of wt-hsa_circ_0013880 with miR-148a-3p mimics or miR-20a-5p mimics inhibited luciferase activity, while no significant alteration was observed in the wt-hsa_circ_0013880 and NC mimic groups (Figure 2F). In addition, these two microRNAs were both downregulated in AML patients (Supplementary Figure S2B,C). In consideration of the above findings, we thus hypothesized that hsa_circ_0013880 might regulate USP32 expression via miR-148a-3p and miR-20a-5p, which may be involved in the development of AML.

Overexpression of hsa_circ_0013880 contributed to the growth of HL-60 cells by regulating USP32

Next, we were interested in whether hsa_circ_0013880 plays a role in AML via regulation of USP32. The hsa_circ_0013880-over-

expressing HL-60 cell line was established via lentivirus infection. Real-time PCR results showed that LV-hsa_circ_0013880 transduction greatly increased the expression of hsa_circ_0013880 in HL-60 cells (Figure 3A). Then, we found that when hsa_circ_0013880 was upregulated, both the mRNA and protein expression levels of USP32 were significantly higher than those in the control cells (Figure 3B,C). As shown in Figure 3D, HL-60 cell viability was significantly increased after hsa_circ_0013880 overexpression but recovered in the cells treated with LV-USP32 shRNA. The proportion of apoptotic cells was markedly reduced in HL-60 cells after overexpression of hsa_circ_0013880 (Figure 3E). However, *USP32* knockdown promoted cell apoptosis in hsa_circ_0013880-overexpressing cells. Consistently, statistical data from the flow cytometric analysis showed the same results in HL-60 cells (Figure 3E). In addition, after upregulation of hsa_circ_0013880, the expression of cyclin D1 was dramatically increased, while the proapoptotic cytokine cleaved caspase-3 was reduced (Figure 3F). Interestingly, the effects of hsa_circ_0013880 on cyclin D1 and cleaved caspase-3 could be reversed by LV-USP32 shRNA. The results displayed in Figure 3G,H showed that LV-Circ + LV-shCtrl-infected HL-60 cells exhibited enhanced migration and colony-forming abilities, which were also inhibited after LV-Circ + LV-USP32sh infection. Consequently, we suggested that overexpression of hsa_circ_0013880 contributed to the survival of HL-60 cells by upregulating USP32.

Knockdown of *USP32* inhibited the proliferation of AML cells

Furthermore, we analysed the effect of USP32 on the proliferation of AML cells. First, the results of real-time PCR and western blot analysis showed that the mRNA and protein levels of USP32 in HL-

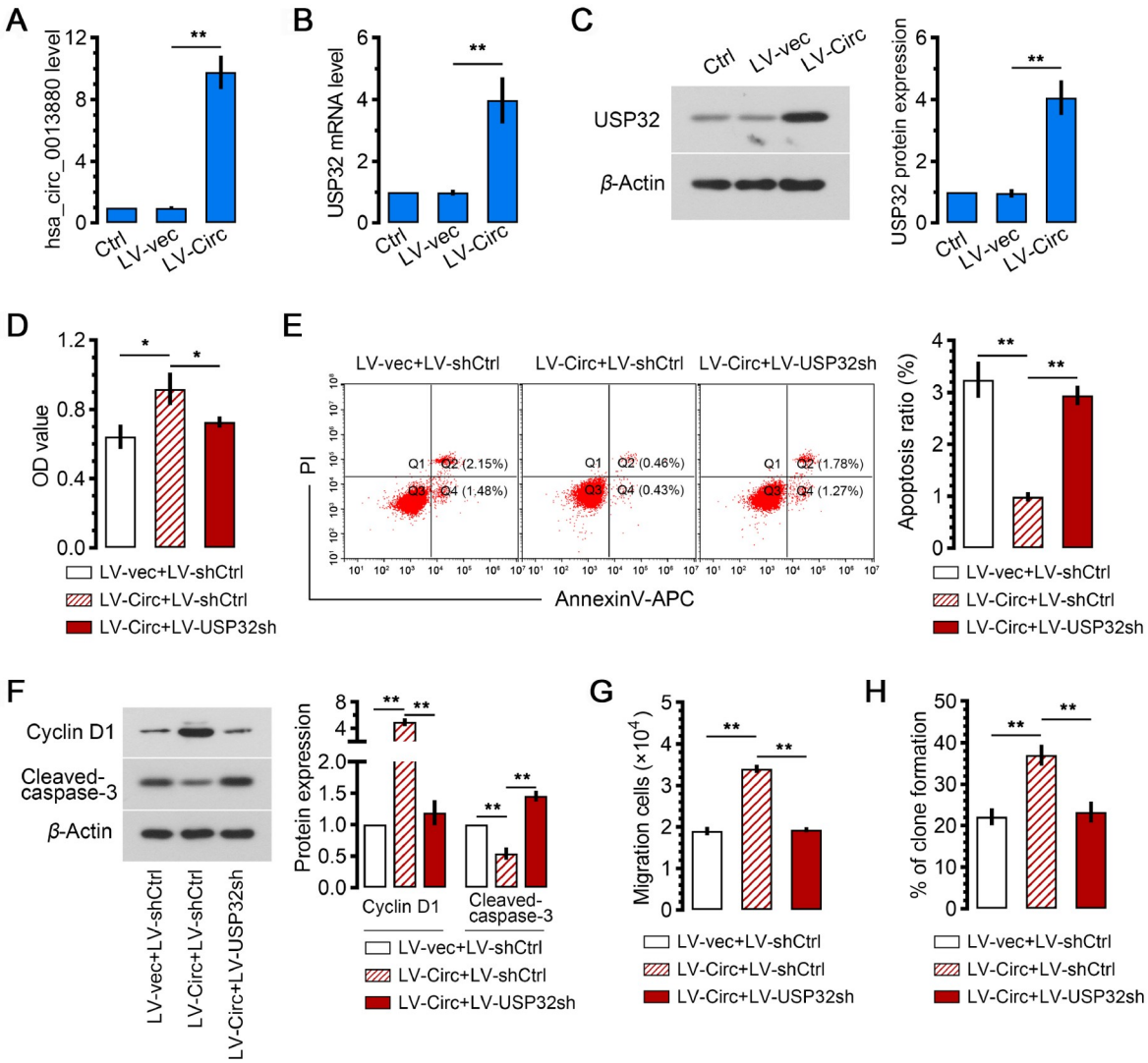

Figure 3. Overexpression of hsa_circ_0013880 enhanced the malignant behaviors of HL-60 cells by increasing the expression of USP32 Cells were infected with hsa_circ_0013880-overexpressing lentiviruses (LV-Circ) and control lentiviruses (LV-vec) for 48 h. (A) Real-time PCR was performed to detect the expression of hsa_circ_0013880. (B,C) The relative expression of USP32 was detected by real-time PCR and western blot analysis. Next, cells were infected with LV-Circ or control LV-vec and USP32 shRNA lentiviruses (LV-USP32sh) or control shRNA lentiviruses (LV-shCtrl) for 48 h. (D) Cell viability was evaluated by CCK-8 assay. (E) Annexin V-APC/PI staining was used to quantitatively analyse early and late cell apoptosis (Q2 and Q4). (F) Western blot analysis of the expressions of Cyclin D1 and cleaved caspase-3 proteins. (G) Transwell migration assay. (H) Colony formation assay. $^{*}P<0.05$ and $^{**}P<0.01$. Data are presented as the mean ± SD. Ctrl, control parental cells.

60 (Figure 4A,B) and U937 (Figure 4E,F) cells were significantly decreased after lentivirus infection (LV-USP32sh#1 and LV-USP32sh#2 groups). Subsequently, CCK-8 assays suggested that downregulation of USP32 expression effectively suppressed the viability of HL-60 (Figure 4C) and U937 (Figure 4G) cells. Similarly, both HL-60 and U937 cells transduced with LV-USP32sh#1 and LV-USP32sh#2 exhibited decreased colony-forming ability (Figure 4D,H). Flow cytometry results revealed that HL-60 and U937 cells were arrested in the G1 phase after *USP32* knockdown (Figure 4I). In addition, the expressions of cyclin D1 and CDK4 were reduced, while P21 was increased in LV-USP32sh#1- and LV-USP32sh#2-infected cells (Figure 4J and Supplementary Figure S2). Hence, we demonstrated that knockdown of *USP32* could inhibit the proliferation of HL-60 and U937 cells, which might be related to cell cycle

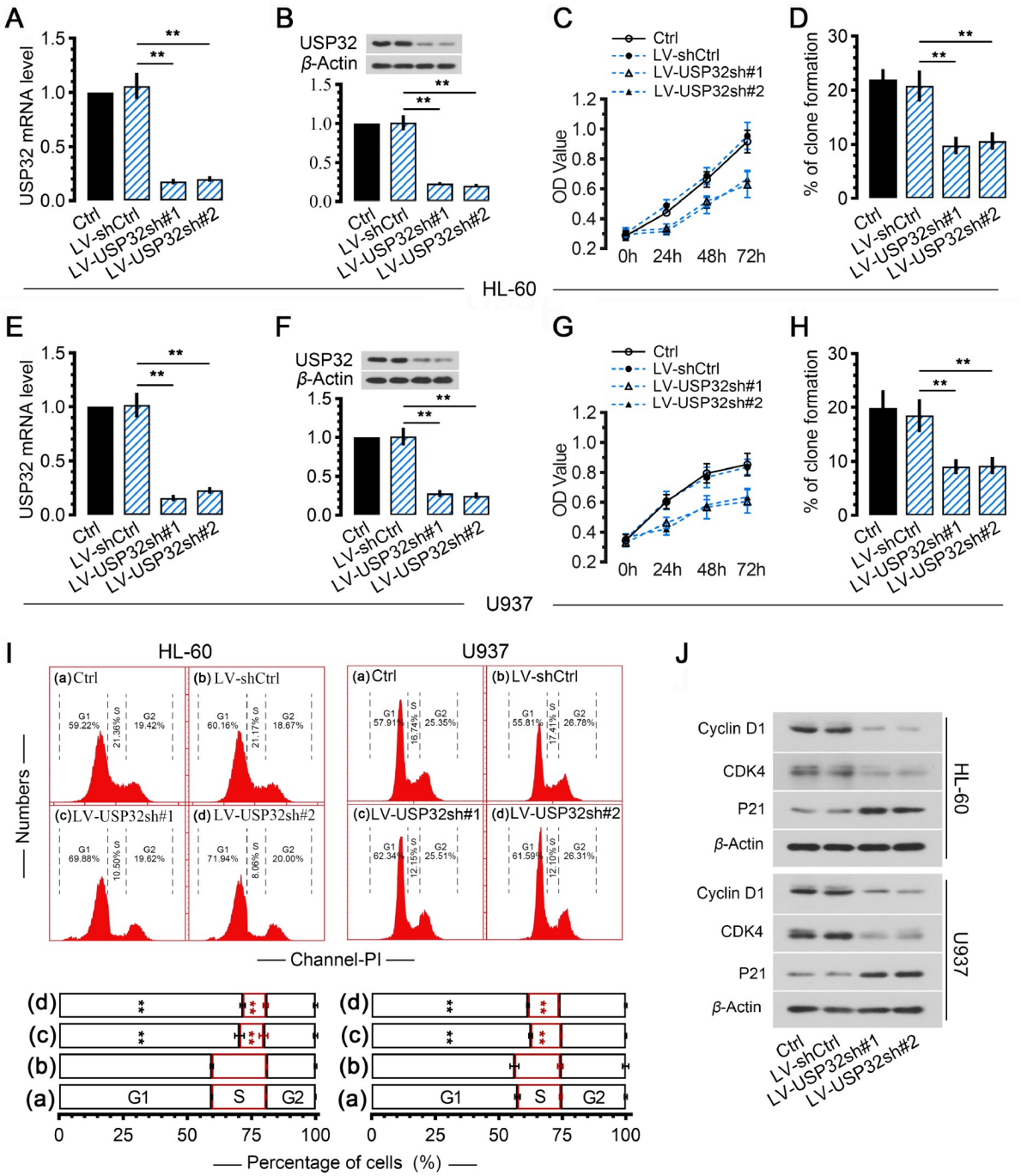

Figure 4. Silencing of *USP32* inhibited the proliferation of AML cells HL-60 and U937 cells were infected with USP32 shRNA lentiviruses (LV-USP32sh#1 and LV-USP32sh#2) or control shRNA lentiviruses (LV-shCtrl) for 48 hours. (A,E) The mRNA levels of USP32 were detected by real-time PCR. (B,F) The expression of USP32 protein was analysed by western blot analysis. (C,G) Cell viability was evaluated by CCK-8 assay. (D,H) Colony formation assay was carried out after infection. (I) The cell cycle was determined by flow cytometry. (J) Western blot analysis of the expressions of Cyclin D1, CDK4 and P21 proteins. $^{**}P < 0.01$. Data are presented as the mean ± SD. Ctrl, control parental cells.

arrest in the G1 phase.

Knockdown of *USP32* promoted apoptosis in AML cells

We further investigated whether USP32 could affect apoptosis in HL-60 and U937 cells. At 48 h after LV-USP32sh#1 and LV-USP32sh#2 treatment, the ratio of apoptotic cells was significantly increased compared with the negative control group (LV-shCtrl) (Figure 5A,B). Consistently, analysis of proteins in cell apoptosis regulation showed that cleaved caspase-3 and -9 and cleaved PARP were increased in *USP32*-silenced cells (Figure 5C and Supplemen-

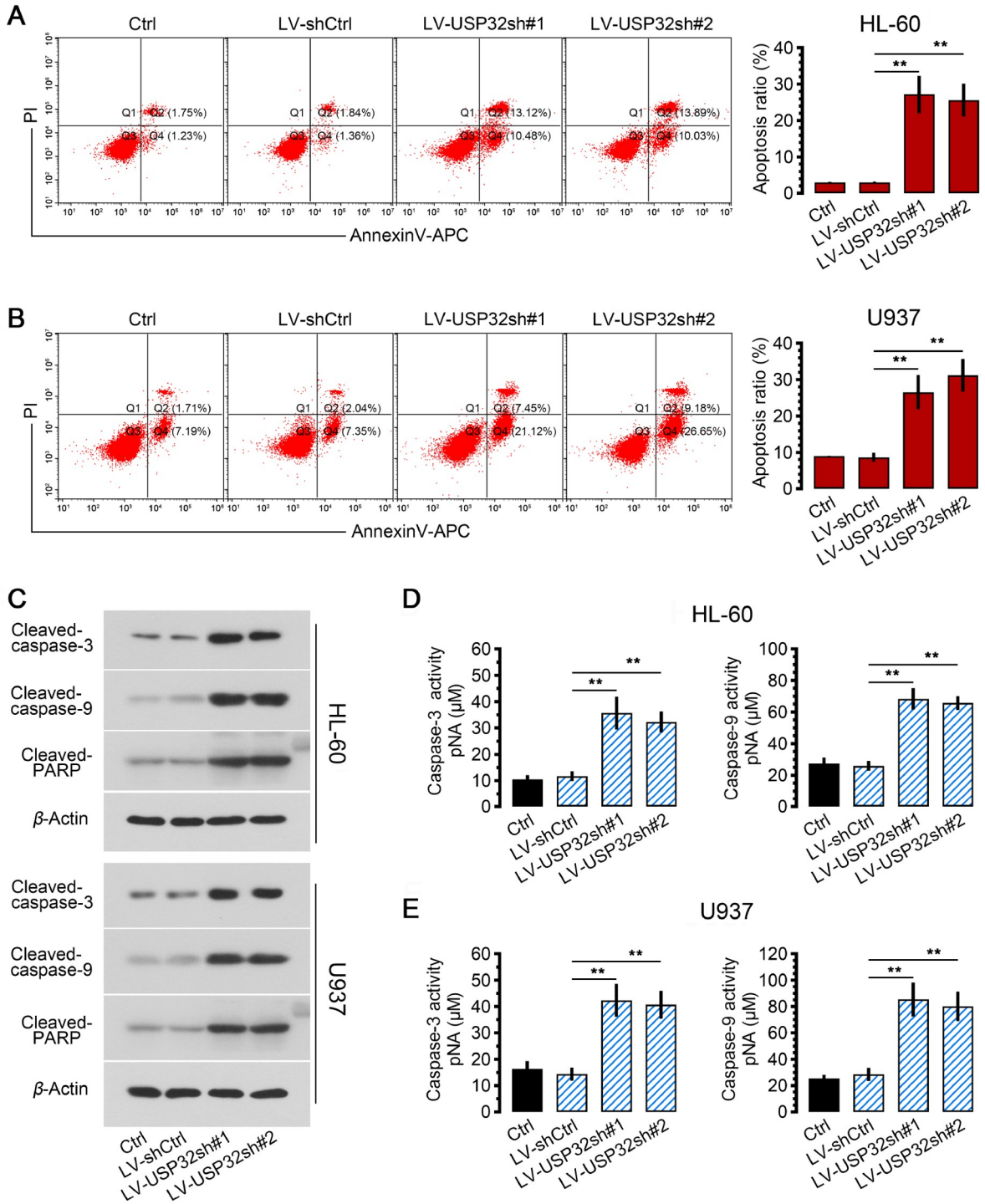

Figure 5. Silencing of *USP32* promoted the apoptosis of AML cells HL-60 and U937 cells were infected with USP32 shRNA lentiviruses (LV-USP32sh#1 and LV-USP32sh#2) or control shRNA lentiviruses (LV-shCtrl) for 48 hours. (A,B) Annexin V-APC/PI staining was used to quantitatively analyse early and late cell apoptosis (Q2 and Q4). (C) The protein levels of cleaved caspase-3, cleaved caspase-9 and cleaved PARP were analysed by western blot analysis. (D,E) The activity of caspase-3 and caspase-9 was estimated by cleavage of the corresponding Ac-DEVD-pNA or Ac-LEVD-pNA to pnitroanilide (pNA). $^{**}P<0.01$. Data are presented as the mean ± SD. Ctrl, control parental cells.

tary Figure S3). The activity of caspase-3 and caspase-9 was obviously enhanced due to *USP32* knockdown (Figure 5D,E). These findings indicated that knockdown of *USP32* could promote the apoptosis of HL-60 and U937 cells.

Knockdown of *USP32* reduced the stability of the Rap1b protein

In addition, we found that Rap1b was upregulated in BMNCs from AML patients (Supplementary Figure S1). Given the deubiquitination function of USP32, we thus presumed that the increase in Rap1b expression might be the consequence of abnormally elevated USP32. Cell experiments showed that Rap1b expression was significantly decreased in HL-60 and U937 cells following *USP32* knockdown (Figure 6A). Coprecipitation of USP32 and Rap1b was also observed in AML cells (Figure 6B). Moreover, by treating cells with the protein synthesis inhibitor CHX (15 μg/mL) for 8 h, we found that the expression of Rap1b protein was decreased in *USP32*-silenced cells (Figure 6C). However, after pretreatment with CHX (15 μg/mL) and the proteasome inhibitor MG132 (10 μM), accumulation of Rap1b was observed in *USP32*-silenced cells, indicating that Rap1b could be regulated by proteasomal degradation. Hence, we hypothesized that USP32 might affect Rap1b expression by controlling its ubiquitination levels. Consistent with its DUB role, *USP32* knockdown markedly increased the level of ubiquitinated Rap1b in AML cells (Figure 6D). In addition, silencing of *hsa_circ_0013880* also contributed to the degradation of Rap1b protein, which might be attributed to the positive regulation of USP32 by hsa_circ_0013880 (Supplementary Figure S4). Accordingly, we demonstrated that knockdown of *USP32* could reduce the stability of the Rap1b protein.

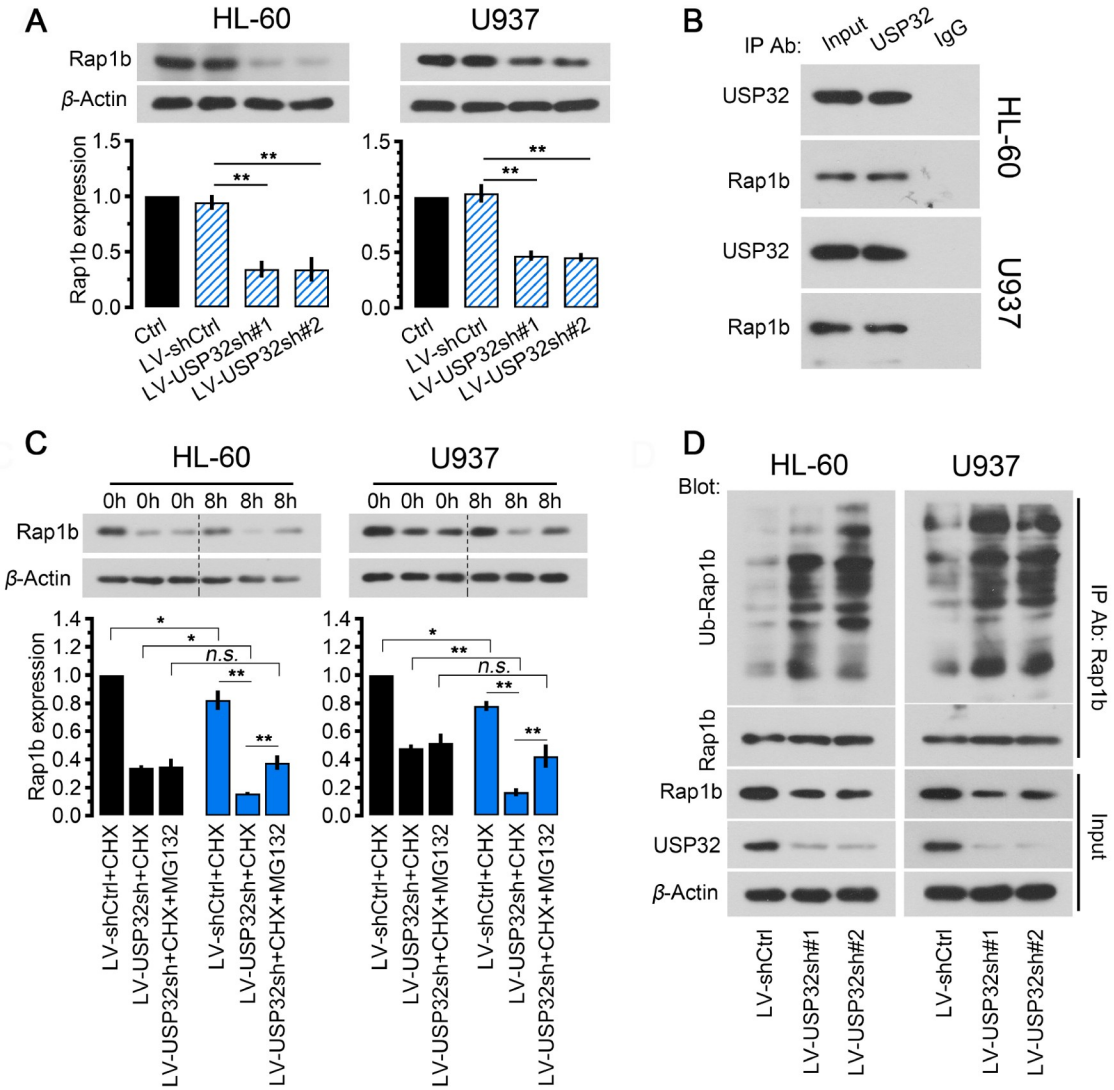

Figure 6. Silencing *USP32* could upregulate the ubiquitination level of Rap1b in AML cells (A) HL-60 and U937 cells were infected with USP32 shRNA lentiviruses (LV-USP32sh#1 and LV-USP32sh#2) or control shRNA lentiviruses (LV-shCtrl) for 48 h. The protein expression of Rap1b was analysed by western blot analysis. (B) Co-IP analyses of USP32 and Rap1b proteins in HL-60 and U937 cells. (C) Western blot analysis of Rap1b expression in AML cells infected with the indicated lentiviral particles and exposed to CHX or treated with MG132 and CHX for 8 h. (D) Ubiquitination assay of Rap1b in HL-60 and U937 cells infected with the indicated lentiviral particles. *$P < 0.05$ and **$P < 0.01$. n.s., no significance. Data are presented as the mean ± SD. Ctrl, control parental cells.

Overexpression of Rap1b reversed the suppression of AML cell survival by *USP32* knockdown

To evaluate whether Rap1b could mediate, at least in part, the effects of USP32 on AML cell growth, we constructed the Rap1b-overexpressing HL-60 cell line (Figure 7A,B). CCK-8 assays confirmed that overexpression of Rap1b increased the viability of *USP32*-silenced HL-60 cells (Figure 7C). In addition, the apoptosis-inducing effects of *USP32* knockdown could be reversed by upregulation of Rap1b (Figure 7D). Next, western blot analysis showed that Rap1b and cyclin D1 expressions were reduced in *USP32*-silenced HL-60 cells, while the cleaved caspase-3 level was increased (Figure 7E,F). However, Rap1b overexpression restored the effects of *USP32* silencing. These results indicated that knockdown of *USP32* could inhibit the growth of HL-60 cells via regulation of Rap1b expression.

Discussion

Studies of AML on genetic characterization have suggested that circRNAs play significant roles in the progression of AML [8,17]. However, the functions of most circRNAs have remained uncertain. Hsa_circ_0013880 has a loop structure without a poly-A tail, which makes it more stable than linear TXNIP. In this study, we showed

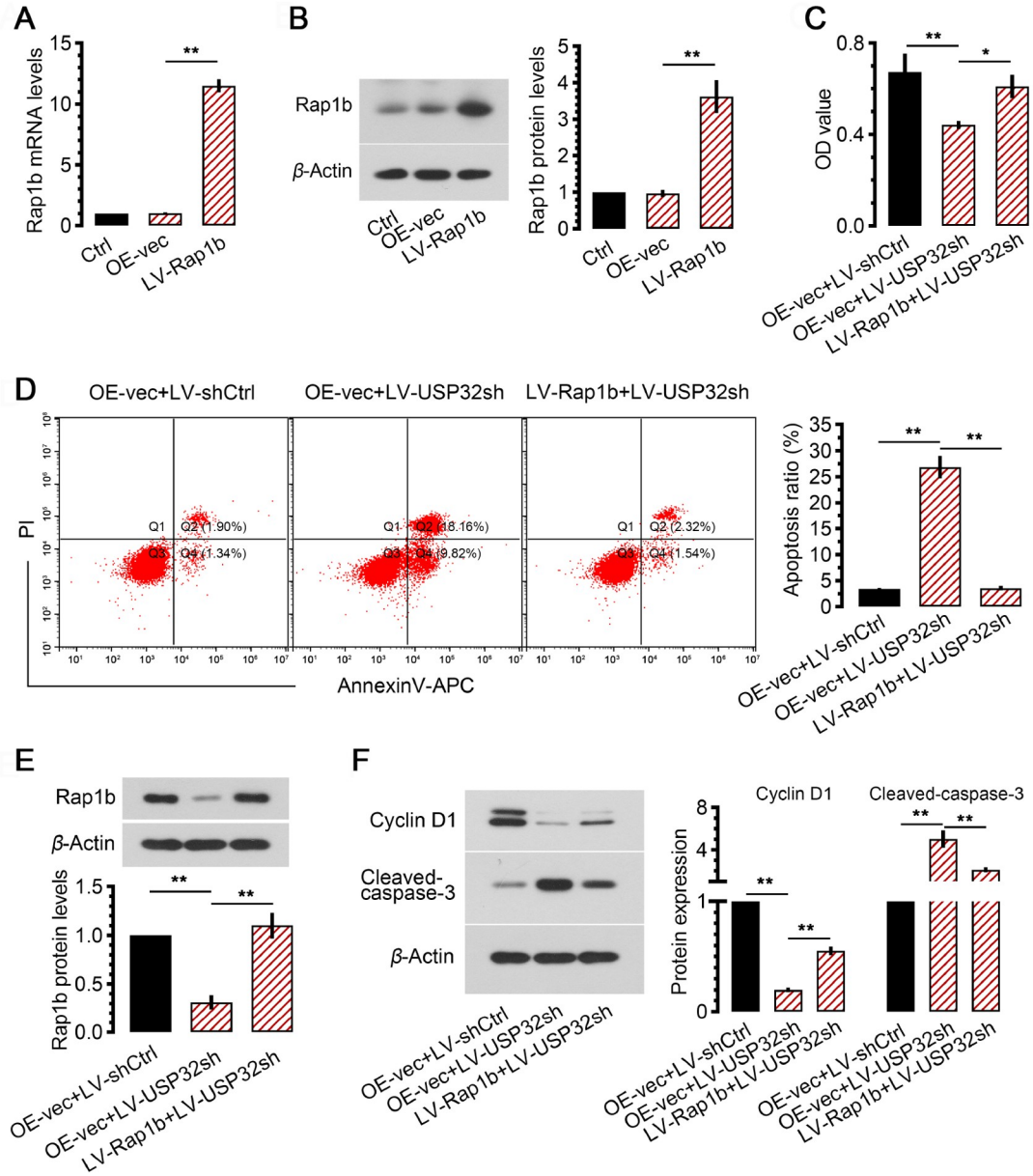

Figure 7. USP32 inhibits the growth of HL-60 cells via regulation of Rap1b (A,B) HL-60 cells were infected with Rap1b-overexpressing lentiviruses (LV-Rap1b) or control lentiviruses (OE-vec) for 48 h. The relative expression of Rap1b was detected by real-time PCR and western blot analysis. Furthermore, cells were infected with LV-Rap1b or OE-vec and USP32 shRNA lentiviruses (LV-USP32sh) or control shRNA lentiviruses (LV-shCtrl) for 48 hours. (C) CCK8 assay was performed to evaluate cell viability. (D) Annexin V-APC/PI staining was used to quantitatively analyse early and late cell apoptosis (Q2 and Q4). (E,F) The protein levels of Rap1b, Cyclin D1 and cleaved caspase-3 were analysed by western blot analysis. $^{*}P<0.05$ and $^{**}P<0.01$. Data are presented as the mean ± SD. Ctrl, control parental cells.

that high hsa_circ_0013880 expression in the BMNCs of AML patients was correlated with high USP32 expression. Further *in vitro* cell experiments revealed that hsa_circ_0013880-mediated elevation of USP32 promoted cell proliferation and migration and reduced cell apoptosis. In addition, *USP32* knockdown inhibited the malignant phenotypes of HL-60 and U937 cells, which might be related to its effect on the ubiquitination level of Rap1b. Therefore, we demonstrated that the hsa_circ_0013880/USP32/Rap1b axis might play an important role in AML progression.

In recent years, high-throughput sequencing analysis confirmed that aberrant expression of microRNAs and circRNAs is associated with many cancers, including AML [18,19]. A previous study reported that circ_0009910 suppresses the proliferation of AML cells through negative regulation of miR-20a-5p [20]. In addition, miR-148a-3p mimics could reduce the cell migration and invasion of J-111 and KG-1a cells, implying that targeting miR-148a-3p might be an effective therapy for AML [21]. According to bioinformatics website predictions, there are microRNA response elements for miR-148a-3p and miR-20a-5p in hsa_circ_0013880, and we validated that hsa_circ_0013880 could bind directly with these two microRNAs in HL-60 cells. Notably, the expression of USP32 was positively regulated by hsa_circ_0013880, and knockdown of *USP32* reversed the cancer-promoting action of hsa_circ_0013880. Interestingly, we found that upregulation of USP32 expression was corrected with miR-148a-3p and miR-20a-5p downregulation. One of the most established mechanisms of action of circRNAs is serving as a "molecular sponge" for microRNAs [22]. For instance, hsa_circ_0003258 acts as a tumor-promoting factor in prostate cancer by sponging miR-653-5p [23]. hsa_circ_0004872 regulates gastric cancer via miR-224-5p [24]. Based on the limited experiments in our study, we proposed a hypothesis that a potential regulatory network among hsa_circ_0013880, miR-148a-3p/miR-20a-5p and USP32 might exist in the development of AML, which may provide a reference for more insightful investigations by other researchers.

USP32 is an ancient and highly conserved gene [25]. Genomic sequencing performed by Chandrasekaran *et al.* [16] revealed that the Tre2 (*USP6*) oncogene was derived from the chimeric fusion of two genes, *USP32* and *TBC1D3*. Studies have demonstrated that *USP32* acts as an oncogene, is expressed in many malignant tumors, and negatively impacts the survival outcome [14,15,26]. Clinically, USP32 expression is abnormally upregulated in epithelial ovarian cancer (EOC). Inhibition of USP32 considerably suppressed the progression of EOC cells [27]. Herein, similar results were also observed in HL-60 and U937 cells. Namely, we found that *USP32* knockdown effectively inhibited HL-60 and U937 cell proliferation, arrested the cell cycle at G1 phase, and induced cell apoptosis.

In addition, the *USP32* gene is an important component of the ubiquitin proteasome system. It was reported that USP32 plays a crucial role in guarding the health of the endolysosomal system by deubiquitination of Rab7 [13]. Thus, we further explored the potential mechanism by which *USP32* knockdown inhibits the growth of AML cells. Rap1b, a small GTPase, can be activated downstream from many surface receptors via guanine nucleotide exchange factors (GEFs) [28] and is upregulated in colorectal cancer, hepatocellular carcinoma and T-acute lymphoblastic leukemia (T-ALL) [29–31]. Functionally, the Rap1b protein participates in many basic biological processes, such as regulating angiogenesis [32], cell adhesion and migration [30,33]. In T-ALL cell lines, Rap1b is required specifically for cell adhesion to the endothelial cell adhesion molecule ICAM-1 [30]. A critical step in T-ALL deterioration is the adhesion of leukemic cells to the endothelium and then transmigration through the endothelium. As a downstream target of miR-28-5p, Rap1b inhibition partially suppressed the oncogenic effect of LINC00514 on pancreatic cancer cells [34]. Herein, our results showed that silencing of *USP32* could increase the ubiquitination level of Rap1b. However, overexpression of Rap1b significantly attenuated the beneficial effects of *USP32* knockdown on AML cells, implying that knockdown of *USP32* could inhibit the growth of HL-60 cells via regulation of Rap1b expression.

In summary, our findings suggest that hsa_circ_0013880 is a novel positive regulator of the proliferation and migration of AML cells through the hsa_circ_0013880/USP32/Rap1b axis. In the future, many *in vitro* and *in vivo* gain-of-function experiments should be carried out to reveal the role of this axis in different kinds of human malignancies.

Supplementary Data

Supplementary data is available at *Acta Biochimica et Biophysica Sinica* online.

Funding

This work was supported by the grants from the Youth Fund Project of the National Natural Science Foundation of China (No. 81900153) and the General Program of Basic Scientific Research Project of Liaoning Provincial Department of Education (No. LJKMZ20221177).

Conflict of Interest

The authors declare that they have no conflict of interest.

References

1. De Kouchkovsky I, Abdul-Hay M. 'Acute myeloid leukemia: a comprehensive review and 2016 update'. *Blood Cancer J* 2016, 6: e441
2. Kantarjian HM, Kadia TM, DiNardo CD, Welch MA, Ravandi F. Acute myeloid leukemia: treatment and research outlook for 2021 and the MD anderson approach. *Cancer* 2021, 127: 1186–1207
3. Shallis RM, Wang R, Davidoff A, Ma X, Zeidan AM. Epidemiology of acute myeloid leukemia: recent progress and enduring challenges. *Blood Rev* 2019, 36: 70–87
4. Pollyea DA, Bixby D, Perl A, Bhatt VR, Altman JK, Appelbaum FR, de Lima M, *et al.* NCCN guidelines insights: acute myeloid leukemia, version 2.2021. *J Natl Comprehensive Cancer Network* 2021, 19: 16–27
5. Kristensen LS, Andersen MS, Stagsted LVW, Ebbesen KK, Hansen TB, Kjems J. The biogenesis, biology and characterization of circular RNAs. *Nat Rev Genet* 2019, 20: 675–691
6. Jamal M, Song T, Chen B, Faisal M, Hong Z, Xie T, Wu Y, *et al.* Recent progress on circular RNA research in acute myeloid leukemia. *Front Oncol* 2019, 9
7. Singh V, Uddin MH, Zonder JA, Azmi AS, Balasubramanian SK. Circular RNAs in acute myeloid leukemia. *Mol Cancer* 2021, 20: 149
8. Li W, Zhong C, Jiao J, Li P, Cui B, Ji C, Ma D. Characterization of hsa_circ_0004277 as a new biomarker for acute myeloid leukemia via circular RNA profile and bioinformatics analysis. *Int J Mol Sci* 2017, 18: 597
9. Salzman J, Chen RE, Olsen MN, Wang PL, Brown PO. Cell-type specific features of circular RNA expression. *PLoS genetics* 2013, 9: e1003777
10. Swatek KN, Komander D. Ubiquitin modifications. *Cell Res* 2016, 26: 399–

422
11. Yau R, Rape M. The increasing complexity of the ubiquitin code. *Nat Cell Biol* 2016, 18: 579–586
12. Clague MJ, Barsukov I, Coulson JM, Liu H, Rigden DJ, Urbé S. Deubiquitylases from genes to organism. *Physiol Rev* 2013, 93: 1289–1315
13. Sapmaz A, Berlin I, Bos E, Wijdeven RH, Janssen H, Konietzny R, Akkermans JJ, *et al.* USP32 regulates late endosomal transport and recycling through deubiquitylation of Rab7. *Nat Commun* 2019, 10: 1454
14. Dou N, Hu Q, Li L, Wu Q, Li Y, Gao Y. USP32 promotes tumorigenesis and chemoresistance in gastric carcinoma via upregulation of SMAD2. *Int J Biol Sci* 2020, 16: 1648–1657
15. Hu W, Wei H, Li K, Li P, Lin J, Feng R. Downregulation of USP32 inhibits cell proliferation, migration and invasion in human small cell lung cancer. *Cell Prolif* 2017, 50: e12343
16. Chandrasekaran AP, Kaushal K, Park CH, Kim KS, Ramakrishna S. USP32 confers cancer cell resistance to YM155 via promoting ER-associated degradation of solute carrier protein SLC35F2. *Theranostics* 2021, 11: 9752–9771
17. Zebisch A, Hatzl S, Pichler M, Wölfler A, Sill H. Therapeutic resistance in acute myeloid leukemia: the role of non-coding RNAs. *Int J Mol Sci* 2016, 17: 2080
18. Wallace JA, O'Connell RM. MicroRNAs and acute myeloid leukemia: therapeutic implications and emerging concepts. *Blood* 2017, 130: 1290–1301
19. Li J, Zhu Z, Li S, Han Z, Meng F, Wei L. Circ_0089823 reinforces malignant behaviors of non-small cell lung cancer by acting as a sponge for microRNAs targeting SOX4. *Neoplasia* 2021, 23: 887–897
20. Ping L, Jian-Jun C, Chu-Shu L, Guang-Hua L, Ming Z. Silencing of circ_0009910 inhibits acute myeloid leukemia cell growth through increasing miR-20a-5p. *Blood Cells Molecules Dis* 2019, 75: 41–47
21. Zhou H, Jia X, Yang F, Shi P. miR-148a-3p suppresses the progression of acute myeloid leukemia via targeting cyclin-dependent kinase 6 (CDK6). *Bioengineered* 2021, 12: 4508–4519
22. Thomson DW, Dinger ME. Endogenous microRNA sponges: evidence and controversy. *Nat Rev Genet* 2016, 17: 272–283
23. Yu YZ, Lv DJ, Wang C, Song XL, Xie T, Wang T, Li ZM, *et al.* Hsa_circ_0003258 promotes prostate cancer metastasis by complexing with IGF2BP3 and sponging miR-653-5p. *Mol Cancer* 2022, 21: 12
24. Ma C, Wang X, Yang F, Zang Y, Liu J, Wang X, Xu X, *et al.* Circular RNA hsa_circ_0004872 inhibits gastric cancer progression via the miR-224/Smad4/ADAR1 successive regulatory circuit. *Mol Cancer* 2020, 19: 157
25. Scanlan MJ, Gordan JD, Williamson B, Stockert E, Bander NH, Jongeneel V, Gure AO, *et al.* Antigens recognized by autologous antibody in patients with renal-cell carcinoma. *Int J Cancer* 1999, 83: 456–464
26. Liu C, Chen Z, Fang M, Qiao Y. MicroRNA let-7a inhibits proliferation of breast cancer cell by downregulating USP32 expression. *Transl Cancer Res* 2019, 8: 1763–1771
27. Nakae A, Kodama M, Okamoto T, Tokunaga M, Shimura H, Hashimoto K, Sawada K, *et al.* Ubiquitin specific peptidase 32 acts as an oncogene in epithelial ovarian cancer by deubiquitylating farnesyl-diphosphate farnesyltransferase 1. *Biochem Biophys Res Commun* 2021, 552: 120–127
28. Chrzanowska-Wodnicka M, Kraus AE, Gale D, White II GC, VanSluys J. Defective angiogenesis, endothelial migration, proliferation, and MAPK signaling in Rap1b-deficient mice. *Blood* 2008, 111: 2647–2656
29. Fan M, Ma X, Wang F, Zhou Z, Zhang J, Zhou D, Hong Y, *et al.* MicroRNA-30b-5p functions as a metastasis suppressor in colorectal cancer by targeting Rap1b. *Cancer Lett* 2020, 477: 144–156
30. Infante E, Heasman SJ, Ridley AJ. Statins inhibit T-acute lymphoblastic leukemia cell adhesion and migration through Rap1b. *J Leukocyte Biol* 2011, 89: 577–586
31. Tang Z, Peng H, Chen J, Liu Y, Yan S, Yu G, Chen Q, *et al.* Rap1b enhances the invasion and migration of hepatocellular carcinoma cells by up-regulating Twist 1. *Exp Cell Res* 2018, 367: 56–64
32. Chrzanowska-Wodnicka M, White GC, Quilliam LA, Whitehead KJ. Small GTPase Rap1 is essential for mouse development and formation of functional vasculature. *PLoS One* 2015, 10: e0145689
33. Jia Z, Yang Y, Dengyan Z, Chunyang Z, Donglei L, Kai W, Song Z. RAP1B, a DVL2 binding protein, activates Wnt/beta-catenin signaling in esophageal squamous cell carcinoma. *Gene* 2017, 611: 15–20
34. Han Q, Li J, Xiong J, Song Z. Long noncoding RNA LINC00514 accelerates pancreatic cancer progression by acting as a ceRNA of miR-28-5p to upregulate Rap1b expression. *J Exp Clin Cancer Res* 2020, 39: 151